The mercury chromates $Hg_6Cr_2O_9$ and $Hg_6Cr_2O_{10}$—Preparation and crystal structures, and thermal behaviour of $Hg_6Cr_2O_9$

Matthias Weil[*], Berthold Stöger

Institute for Chemical Technologies and Analytics, Division of Structural Chemistry, Vienna University of Technology, Getreidemarkt 9/164-SC, A-1060 Vienna, Austria

Abstract

The basic mercury(I) chromate(VI), $Hg_6Cr_2O_9$ ($= 2Hg_2CrO_4 \cdot Hg_2O$), has been obtained under hydrothermal conditions (200 °C, 5 days) in the form of orange needles as a by-product from reacting elemental mercury and $K_2Cr_2O_7$. Hydrothermal treatment of microcrystalline $Hg_6Cr_2O_9$ in demineralised water at 200 °C for 3 days led to crystal growth of red crystals of the basic mercury(I, II) chromate(VI), $Hg_6Cr_2O_{10}$ ($= 2Hg_2CrO_4 \cdot 2HgO$). The crystal structures were solved and refined from single crystal X-ray data sets. $Hg_6Cr_2O_9$: space group $P2_12_12_1$, $Z = 4$, $a = 7.3573(12)$, $b = 8.0336(13)$, $c = 20.281(3)$ Å, 3492 structure factors, 109 parameters, $R[F^2 > 2\sigma(F^2)] = 0.0371$, $wR(F^2$ all$) = 0.0517$; $Hg_6Cr_2O_{10}$: space group $Pca2_1$, $Z = 4$, $a = 11.4745(15)$, $b = 9.4359(12)$, $c = 10.3517(14)$ Å, 3249 structure factors, 114 parameters, $R[F^2 > 2\sigma(F^2)] = 0.0398$, $wR(F^2$ all$) = 0.0625$. Both crystal structures are made up of an intricate mercury–oxygen network, subdivided into single building blocks [O–Hg–Hg–O] for the mercurous compound, and [O–Hg–Hg–O] and [O–Hg–O] for the mixed-valent compound. $Hg_6Cr_2O_9$ contains three different Hg_2^{2+} dumbbells, whereas $Hg_6Cr_2O_{10}$ contains two different Hg_2^{2+} dumbbells and two Hg^{2+} cations. The Hg^I–Hg^I distances are characteristic and range between 2.5031(15) and 2.5286(9) Å. All Hg_2^{2+} groups exhibit an unsymmetrical oxygen environment. The oxygen coordination of the Hg^{2+} cations is nearly linear with two tightly bonded O atoms at distances around 2.07 Å. For both structures, the chromate(VI) anions reside in the vacancies of the Hg–O network and deviate only slightly from the ideal tetrahedral geometry with average Cr–O distances of ca. 1.66 Å. Upon heating at temperatures above 385 °C, $Hg_6Cr_2O_9$ decomposes in a four-step mechanism with Cr_2O_3 as the end-product at temperatures above 620 °C.

© 2006 Elsevier Inc. All rights reserved.

Keywords: Mercury; Chromates; $Hg_6Cr_2O_9$; $Hg_6Cr_2O_{10}$; Crystal structure; Thermal behaviour

1. Introduction

In the past decade, the syntheses and crystal chemistry of complex oxocompounds have been reported that contain mercury in the fractional oxidation state of $+IV/3$ under formation of the trigonal cluster cation Hg_3^{4+}. These compounds are of considerable interest owing to the unusual electronic situation of the Hg_3^{4+} cation with its two-electron–three-centre bonding ($2e$–$3c$). The peculiar structural motif of an Hg_3^{4+} triangle is realised in the minerals *terlinguaite*, $(Hg_3)(HgO_2)Cl_2$ [1], and *kuznetsovite*, $(Hg_3)AsO_4Cl$ [2,3], and in the isotypic P and Br analogues

of *kuznetsovite*, $(Hg_3)PO_4Cl$ and $(Hg_3)AsO_4Br$ [3]. Other synthetic representatives containing Hg_3^{4+} clusters are the isotypic arsenate and phosphate, $(Hg_3)_3(AsO_4)_4$ [4] and $(Hg_3)_3(PO_4)_4$ [5], respectively, as well as the basic phosphate $(Hg_3)_2(HgO_2)(PO_4)_2$ [5]. Crystals of these compounds were grown by taking advantage of the synproportionation reaction between different mercury species, viz. Hg, Hg_2^{2+} and Hg^{2+} (Eqs. (1) and (2)):

$$2Hg^{2+} + Hg = Hg_3^{4+}, \tag{1}$$

$$Hg_2^{2+} + Hg^{2+} = Hg_3^{4+}. \tag{2}$$

Preparation of the mixed-valent mercury selenium oxocompounds $Hg_7Se_3O_{13}H_2$ and $Hg_8Se_4O_{17}H_2$ [6], both comprising Hg_2^{2+} dumbbells, Hg_3^{4+} triangles, Hg^{2+}

*Corresponding author. Fax: +43 1 58801 17199.

E-mail address: mweil@mail.zserv.tuwien.ac.at (M. Weil).

cations, HgO_2^{2-} dumbbells, trigonal-pyramidal SeO_3^{2-} and tetragonal SeO_4^{2-} entities, has shown that the redox equilibria (Eqs. (1) and (2)) can be affected by other redox-pairs, in this case by Se^{IV}/Se^{VI}. Other possible redox-pairs with an influence on Eqs. (1) and (2) include chromium with its various (more or less stable) oxidation states. Moreover, the mineral *wattersite*, $Hg_5CrO_6 (= (Hg_2)_2HgO_2(CrO_4))$, contains chromate(VI) anions and mixed-valent mercury with crystal-chemical functions as Hg_2^{2+} and Hg^{2+} groups [7]. From there it appears possible that the formation of the trigonal cluster cation Hg_3^{4+} (Eq. (2)) might be achieved in principle in the system Hg–Cr–O–H, and we started to re-investigate the formation, crystal growth and thermal behaviour of phases in this system.

Numerous mercury chromates with different oxidation states of both mercury and chromium have been listed in one of the older handbooks on chromium and its compounds [8]. In the meantime, some of these phases have been structurally characterised which, besides *wattersite*, comprise the mercury(II) chromates(VI) in the form of the double basic salt $HgCrO_4 \cdot 2HgO$ (single crystal X-ray diffraction) [9], the neutral salt $HgCrO_4$ (single crystal X-ray diffraction) [10], and the hemihydrate $HgCrO_4 \cdot \frac{1}{2}H_2O$ (single crystal neutron diffraction) [11]. The spinel-type $HgCr_2O_4$ is the only representative for a mercury(II) chromate(III) (X-ray powder diffraction) [12]. During our recent study, several new compounds were obtained and structurally characterised by single-crystal X-ray diffraction, including the mercury(II) dichromate(VI), $HgCr_2O_7$ [13], a second modification of $HgCrO_4$ and the monohydrate $HgCrO_4 \cdot H_2O$ [14], as well as $HgCr_2O_4$, the structure of which was re-determined [15]. In the course of these systematic investigations, crystals of two new mercury chromates were successfully grown: the basic mercury(I) chromate(VI), $Hg_6Cr_2O_9$, and the mixed-valent mercury(I) mercury(II) chromate(VI), $Hg_6Cr_2O_{10}$. In this communication, we report on the preparation conditions and crystal structures for both compounds, as well as on the thermal behaviour of $Hg_6Cr_2O_9$.

2. Experimental

2.1. Preparation

All chemicals used were purchased from Merck (analytical grade). Single crystals of $Hg_6Cr_2O_9$ were obtained under hydrothermal conditions. In a typical experiment elemental Hg (3.371 g, 16.8 mmol) and $K_2Cr_2O_7$ (74 mg, 0.3 mmol) were mixed in a 10 ml Teflon inlay filled with 6 ml demineralised water. Two drops of 65 wt% nitric acid were added, resulting in an immediate formation of a brown precipitate which was not further analysed. The Teflon inlay was placed in a steel autoclave and heated at 200 °C for 5 days. Besides unreacted mercury, the obtained solid consisted of a mixture of different products, including major amounts of a dark-red to black powder, few orange

needle-like crystals of $Hg_6Cr_2O_9$, and few red plates of synthetic *wattersite*. X-ray powder diffraction (XRPD) of the bulk revealed $HgCrO_4 \cdot 2HgO$ as the main phase, besides traces of a yet unidentified phase in the system Hg–Cr–O–(H).

Hydrothermal treatment of microcrystalline $Hg_6Cr_2O_9$ (100 mg) in a 5 ml Teflon inlay filled with 3 ml demineralised water at 200 °C for 3 days led to single crystal growth of dark-red blocks of synthetic *wattersite* and few red crystals of $Hg_6Cr_2O_{10}$, the latter being frequently aggregated to rosettes. No additional phases were identified by XRPD of the bulk material.

Microcrystalline $Hg_6Cr_2O_9$ was prepared by precipitation of a slightly acidified solution of $Hg_2(NO_3)_2 \cdot 2H_2O$ (4.4 mmol) in 16 ml water with 171 mg (1.1 mmol) K_2CrO_4 dissolved in 4 ml demineralised water. The red suspension was refluxed for 4 h and vacuum filtered to give a colourless filtrate and a bright red powder which was washed with water and an acetone/ethanol mixture and finally dried in a desiccator overnight. XRPD revealed $Hg_6Cr_2O_9$ as a single phase.

Attempts to obtain the mixed-valent compound $Hg_6Cr_2O_{10}$ in microcrystalline form by precipitation of solutions containing Hg^{2+} and Hg_2^{2+} in various stoichiometric ratios and with varying chromate concentrations were not successful. These experiments led also to $Hg_6Cr_2O_9$ when working with a lower chromate concentration, or to mixtures of $Hg_6Cr_2O_9$, $HgCrO_4 \cdot 2HgO$, synthetic *wattersite* and minor amounts of yet unknown phase(s) in more concentrated chromate solutions.

2.2. X-ray powder diffraction (XRPD)

Measurements of the ground bulk products were performed on a Philips X'Pert Pro diffractometer system (Cu-$K\alpha_{1,2}$ radiation ($\lambda = 1.54060$, $1.54439\,Å$), Bragg–Brentano geometry, silicon single crystal sample holder, 5–70° 2θ, 0.02°/step, 5s/step).

2.3. Single crystal diffraction

Single crystals of $Hg_6Cr_2O_{10}$ suitable for measurement were broken from a larger rosette-shaped aggregate. The optical quality of selected crystals was checked under a polarising microscope. X-ray diffraction intensities of the single crystals were collected at 22 °C using the ω-scan technique with 0.3° rotation width and 35 s exposure time per frame on a SMART APEX three-circle diffractometer equipped with a CCD camera (Bruker AXS; Mo $K\bar{\alpha}$ radiation, $\lambda = 0.71073\,Å$). Three independent sets of 600 frames were measured thus scanning the whole reciprocal sphere with high redundancy. The measured intensities were corrected for Lorentz and polarisation effects, and a numerical absorption correction was applied by optimisation of the crystal shape using the program HABITUS [16]. The crystal structures were solved by direct methods and refined with the SHELXTL program package [17]. In the

Table 1
Details of data collection and structure refinement

Compound	$Hg_6Cr_2O_9$	$Hg_6Cr_2O_{10}$
Crystal dimensions [mm]	0.110···0.035···0.015	0.024···0.018···0.012
Crystal colour; shape	Orange; needle	Red; fragment
Crystal system	Orthorhombic	Orthorhombic
Space group (no.)	$P2_12_12_1$ (19)	$Pca2_1$ (29)
Formula units Z	4	4
a [Å]	7.3573(12)	11.4745(15)
b [Å]	8.0336(13)	9.4359(12)
c [Å]	20.281(3)	10.3517(14)
V [Å^3]	1198.7(3)	1120.8(3)
Formula weight [g mol^{-1}]	1451.54	1467.54
μ [mm^{-1}]	78.303	83.756
X-ray density [g cm^{-3}]	8.043	8.697
Range θ_{min}–θ_{max} [deg]	2.01–29.99	2.16–30.00
Range		
h	$-10 \rightarrow 10$	$-15 \rightarrow 15$
k	$-11 \rightarrow 11$	$-13 \rightarrow 11$
l	$-28 \rightarrow 28$	$-14 \rightarrow 14$
Measured reflections	13530	11850
Independent reflections	3492	3249
Obs.reflections [$I > 2\sigma(I)$]	2637	2282
R_i	0.077	0.071
Trans. coef. T_{min}; T_{max}	0.1272; 0.6416	0.1051; 0.4148
Number of parameters	109	114
Diff. elec. dens. max.; min [e$^-$ Å^{-3}] (distance [Å], atom)	3.35 (0.05, Hg6); -1.68 (0.57, Hg2)	3.35 (0.67, Hg5) -2.96 (0.75, Hg5)
Flack parameter, number of Friedel pairs	$-0.01(2)$, 1468	0.24(3), 1528
$R[F^2 > 2\sigma(F^2)]$	0.0371	0.0398
w$R_2(F^2$ all)	0.0517	0.0625
Goof	0.798	0.838
CSD number	416208	416209

last least-squares cycles the thermal displacement parameters of the heavy atoms were refined anisotropically while those of the oxygen atoms were refined isotropically. The final difference Fourier maps did not indicate any additional atomic sites, and the highest difference peaks were located close to the mercury positions. The structural parameters were standardised using the program STRUC-TURE-TIDY [18]. Analysis of the refined atomic coordinates with the program PLATON [19] did not reveal any higher symmetry. Moreover, for the structure of $Hg_6Cr_2O_9$, the refined Flack parameter [20] of $-0.01(2)$ using 1468 Friedel pairs gave a clear indication of the absence of a centre of symmetry, while for $Hg_6Cr_2O_{10}$ partial inversion twinning had to be considered, resulting in a Flack parameter of 0.24(3) using 1528 Friedel pairs.

Further details of data collection and structure refinement are summarised in Table 1. Final atomic coordinates and equivalent isotropic displacement parameters are listed in Table 2, and selected interatomic distances and angles are given in Table 3. Additional crystallographic information on both structures is available from the Fachinformationszentrum Karlsruhe, D-76344 Eggenstein-Leopoldshafen, Germany, email: crysdata@fiz-karlsruhe.de, by quoting the literature citation, the name of the authors and the depository number listed at the end of Table 1. Drawings of structural details were produced using the program ATOMS [21].

Thermoanalytical measurements were performed in an open system under a flowing N_2 atmosphere on a Mettler-Toledo TG50 (35–800 °C, heating rate 5 °C min^{-1}, corundum crucibles) and a Mettler-Toledo DSC 25 system (35–550 °C, heating rate 5 °C min^{-1}, aluminium capsules).

3. Results and discussion

3.1. Formation

A systematic investigation on the formation conditions of phases in the pseudobinary system Hg_2O–CrO_3 was published nearly hundred years ago [22]. These studies report three different mercurous chromates: The neutral salt, Hg_2CrO_4, and the two basic salts, $Hg_8Cr_3O_{13}$ ($= 3Hg_2CrO_4 \cdot Hg_2O$) and $Hg_6Cr_2O_9$ ($= 2Hg_2CrO_4 \cdot Hg_2O$). The neutral salt was reported to be obtained by precipitation of mercurous nitrate with stoichiometric amounts of potassium chromate in slightly acidified solutions. The precipitate is amorphous in the cold, but crystallises after some minutes, or immediately when heated in the mother liquor. The salt $Hg_8Cr_3O_{13}$ formed during hydrolysis of amorphous Hg_2CrO_4 with cold water, while $Hg_6Cr_2O_9$ was produced when Hg_2CrO_4 was boiled in an excess of a mercurous nitrate solution.

Our experimental results confirm the formation of the neutral salt Hg_2CrO_4 and of the basic $Hg_6Cr_2O_9$, whereas

Table 2
Atomic coordinates and isotropic displacement parameters [Å^2]. All atoms are on general positions 4a

Atom	x	y	z	U_{eq} [a]
Hg₆Cr₂O₉				
Hg1	0.01976(9)	0.02634(8)	0.45468(3)	0.02873(17)
Hg2	0.10345(9)	0.78303(8)	0.30693(3)	0.02703(16)
Hg3	0.11681(9)	0.24748(8)	0.53612(3)	0.02585(15)
Hg4	0.21486(8)	0.68700(9)	0.19559(3)	0.02711(16)
Hg5	0.40729(9)	0.35165(8)	0.11998(3)	0.02638(15)
Hg6	0.53471(9)	0.06377(8)	0.13756(4)	0.03207(18)
Cr1	0.0260(3)	0.0860(3)	0.05888(13)	0.0250(6)
Cr2	0.2991(3)	0.1900(3)	0.29846(12)	0.0184(5)
O1	0.0191(13)	0.2850(13)	0.0950(5)	0.028(3)
O2	0.1267(13)	0.0888(12)	0.3348(5)	0.021(2)
O3	0.1823(16)	0.5214(16)	0.4498(6)	0.048(4)
O4	0.2240(14)	0.3121(13)	0.2403(5)	0.027(3)
O5	0.2733(12)	0.5817(12)	0.1032(5)	0.020(2)
O6	0.3611(16)	0.0402(16)	0.6057(6)	0.048(4)
O7	0.4148(16)	0.3074(14)	0.3555(6)	0.041(3)
O8	0.4368(15)	0.0537(14)	0.2674(6)	0.033(3)
O9	0.6222(15)	0.4043(15)	0.0106(6)	0.046(3)
Hg₆Cr₂O₁₀				
Hg1	0.09386(8)	0.57356(10)	0.41016(7)	0.0257(2)
Hg2	0.24762(11)	0.26437(8)	0.32876(15)	0.01933(15)
Hg3	0.40485(9)	0.66736(10)	0.24688(10)	0.0344(3)
Hg4	0.41154(5)	0.24522(10)	0.07802(15)	0.01850(14)
Hg5	0.61527(10)	0.16261(12)	0.40172(14)	0.0498(4)
Hg6	0.88023(8)	0.06711(10)	0.25969(8)	0.0252(2)
Cr1	0.1357(2)	0.0541(3)	0.0800(3)	0.0154(6)
Cr2	0.1447(2)	0.5494(3)	0.0793(3)	0.0130(5)
O1	0.0207(13)	0.5038(17)	0.1587(14)	0.024(4)
O2	0.0921(10)	0.3466(15)	0.3988(13)	0.013(3)
O3	0.1331(11)	0.233(2)	0.078(3)	0.041(4)
O4	0.1378(11)	0.0037(14)	0.2323(15)	0.023(4)
O5	0.2541(15)	0.0073(15)	0.0002(14)	0.027(3)
O6	0.2616(13)	0.4865(14)	0.1510(13)	0.021(3)
O7	0.3608(10)	0.4954(14)	0.4263(16)	0.019(3)
O8	0.3932(11)	0.1632(16)	0.2617(15)	0.021(4)
O9	0.5178(12)	0.0072(16)	0.0035(13)	0.015(3)
O10	0.6496(10)	0.2747(15)	0.083(2)	0.030(3)

[a] U_{eq} is defined as one third of the trace of the orthogonalized U_{ij} tensor.

the phase Hg$_8$Cr$_3$O$_{13}$ has not been observed. Depending on the hydrolysation grade of the neutral salt with ice water, we always obtained phase mixtures of Hg$_6$Cr$_2$O$_9$ and Hg$_2$CrO$_4$ in varying ratios, as identified by XRPD. Thus it is most likely that the authors in [22] have analysed a phase mixture close to a ratio Hg$_2$CrO$_4$:Hg$_6$Cr$_2$O$_9$ = 1:1, which would explain the derived formula Hg$_8$Cr$_3$O$_{13}$ (= Hg$_2$CrO$_4$ + Hg$_6$Cr$_2$O$_9$).

We have also obtained Hg$_6$Cr$_2$O$_9$ at room temperature from precipitation of a mixture of mercurous and mercuric nitrate solutions with diluted chromate solutions. The product formation indicates a lower solubility of the mercurous phase compared to mixed-valent mercury phases or mercuric phases. The formation of Hg$_6$Cr$_2$O$_9$ single crystals was only achieved by oxidising elemental mercury with a diluted dichromate solution under hydrothermal conditions. These experiments yielded Hg$_6$Cr$_2$O$_9$

crystals, besides Hg$_5$CrO$_6$ (*wattersite*) with mixed-valent mercury and the basic mercuric salt HgCrO$_4$ · 2HgO. The co-existence of several mercury phases with different oxidation states in one batch is evidence of a complex interplay of various redox-, hydrolysis- and precipitation equilibria taking place under these conditions. Similar observations of multiphase formation with different oxidation states for mercury and/or the accompanying anions have been made during hydrothermal phase formation experiments in the system Hg–Se–O–H [6,23]. Multiphase formation was also observed during hydrothermal treatment of microcrystalline Hg$_6$Cr$_2$O$_9$ in demineralised water. The employed Hg$_6$Cr$_2$O$_9$ first hydrolyses under liberation of chromate which, under the given neutral or only slightly acidic conditions, has a much lower oxidising effect than in acid solutions.[1] This leads to only a partial oxidation of Hg$_2^{2+}$ to Hg^{2+}, resulting in the mixed-valent phases Hg$_6$Cr$_2$O$_{10}$ and Hg$_5$CrO$_6$ (*wattersite*). The slight green colour of the remaining solutions after completion of the experiments showed the presence of hydrated Cr^{3+} ions. However, we did not observe solid phases with chromium in oxidation state +III under these conditions.

3.2. Structures

Recent reviews on the crystal chemistry of mercury include compounds with mercury in lower oxidation states < II [25], structural peculiarities of various mercury oxo- and chalcohalides [26], and details of structural fragmentation and packing in the then known mercury chromates [27].

Both Hg$_6$Cr$_2$O$_9$ and Hg$_6$Cr$_2$O$_{10}$ crystallise in new structure types. They consist of an intricate mercury-oxygen network with the chromate(VI) anions residing in the vacancies (Figs. 1,3). In the mercurous compound, Hg$_6$Cr$_2$O$_9$, there are three crystallographically independent Hg$_2^{2+}$ dumbbells, whereas the mixed-valent Hg$_6$Cr$_2$O$_{10}$ contains two different Hg$_2^{2+}$ dumbbells and two Hg^{2+} cations. The Hg^I–Hg^I distances are characteristic for monovalent mercury and range between 2.5031(15) and 2.5286(9) Å which is in very good agreement with the average distance of 2.518(25) Å calculated for more than 100 independent Hg$_2^{2+}$ groups observed for various inorganic oxocompounds [28]. All Hg$_2^{2+}$ groups are built of two inequivalent Hg atoms which results in an unsymmetrical oxygen environment. Besides the neighbouring Hg atom in each dumbbell, the mercury atoms are coordinated by three to five additional oxygen atoms if interactions between mercury and oxygen are considered as bonding for Hg–O distances < 3.1 Å. Another characteristic feature for mercurous oxocompounds concerns the formation of single building blocks [O–Hg–Hg–O] with

---

[1] The standard reduction potential E^0 for the reaction HCrO$_4^-$ + 7H$^+$ + 3e$^-$ = Cr^{3+} + 4 H$_2$O is 1.350 V, whereas that of the reaction CrO$_4^{2-}$ + 4 H$_2$O + 3e$^-$ = Cr(OH)$_3$ + 5 OH$^-$ is −0.13 V [24].

Table 3
Selected distances [Å] and angles [deg]

Hg₆Cr₂O₉

Hg1	O1	2.204(10)	Hg4	O5	2.100(10)	Cr1	O9	1.578(12)	
Hg1	O5	2.495(9)	Hg4	Hg2	2.5230(10)	Cr1	O6	1.619(13)	
Hg1	Hg3	2.5286(9)	Hg4	O2	2.705(10)	Cr1	O3	1.628(12)	
Hg1	O2	2.603(10)	Hg4	O8	2.877(11)	Cr1	O1	1.759(10)	
Hg1	O9	2.898(11)	Hg4	O6	2.905(13)	av.		1.646	
Hg2	O1	2.184(10)	Hg5	O5	2.122(10)	Cr2	O8	1.620(11)	
Hg2	Hg4	2.5230(10)	Hg5	Hg6	2.5208(9)	Cr2	O4	1.631(11)	
Hg2	O2	2.526(10)	Hg5	O9	2.757(12)	Cr2	O2	1.678(10)	
Hg2	O4	2.603(10)	Hg5	O4	2.806(10)	Cr2	O7	1.719(12)	
Hg3	O5	2.095(9)	Hg5	O1	2.950(10)	av.		1.662	
Hg3	Hg1	2.5286(9)	Hg5	O8	3.028(11)				
Hg3	O7	2.689(11)	Hg6	O7	2.098(12)	O9	Cr1	O6	109.0(6)
Hg3	O6	2.828(12)	Hg6	Hg5	2.5208(9)	O9	Cr1	O3	109.9(6)
Hg3	O3	2.852(13)	Hg6	O8	2.730(11)	O6	Cr1	O3	110.3(6)
			Hg6	O3	2.755(12)	O9	Cr1	O1	109.9(6)
			Hg6	O6	3.098(12)	O6	Cr1	O1	109.9(6)
						O3	Cr1	O1	107.9(6)
O1	Hg1	Hg3	162.4(3)			O8	Cr2	O4	109.7(5)
O1	Hg2	Hg4	162.1(3)			O8	Cr2	O2	108.4(5)
O5	Hg3	Hg1	173.5(3)			O4	Cr2	O2	110.7(5)
O5	Hg4	Hg2	171.2(3)			O8	Cr2	O7	108.9(6)
O5	Hg5	Hg6	174.0(3)			O4	Cr2	O7	109.0(6)
O7	Hg6	Hg5	167.5(3)			O2	Cr2	O7	110.1(5)
Hg3	O5	Hg4	113.3(4)						
Hg3	O5	Hg5	119.7(4)						
Hg4	O5	Hg5	107.6(4)						
Hg3	O5	Hg1	98.3(4)						
Hg4	O5	Hg1	108.3(4)						
Hg5	O5	Hg1	108.7(4)						

Hg₆Cr₂O₁₀

|									
Hg1	O2	2.145(14)	Hg4	O8	2.064(16)	Cr1	O4	1.647(16)	
Hg1	Hg5	2.5031(15)	Hg4	O2	2.088(14)	Cr1	O5	1.651(17)	
Hg1	O7	2.758(11)	Hg4	O9	2.669(15)	Cr1	O9	1.671(14)	
Hg1	O1	2.813(15)	Hg4	O10	2.746(12)	Cr1	O3	1.692(19)	
Hg1	O1	2.980(15)	Hg4	O1	2.806(16)	av.		1.665	
Hg1	O6	3.105(13)	Hg4	O6	2.952(14)	Cr2	O6	1.644(15)	
Hg2	O8	2.045(13)	Hg5	O4	2.367(15)	Cr2	O10	1.661(15)	
Hg2	O2	2.077(13)	Hg5	O5	2.420(16)	Cr2	O7	1.666(17)	
Hg2	O7	2.731(13)	Hg5	O9	2.451(14)	Cr2	O1	1.699(15)	
Hg2	O6	2.794(14)	Hg5	Hg1	2.5031(15)	av.		1.668	
Hg2	O3	2.93(3)	Hg5	O8	2.932(14)				
Hg2	O3	2.93(3)	Hg6	O8	2.178(15)	O4	Cr1	O5	112.9(7)
Hg3	O1	2.282(15)	Hg6	Hg3	2.5248(13)	O4	Cr1	O9	111.4(7)
Hg3	O7	2.517(15)	Hg6	O9	2.839(13)	O5	Cr1	O9	109.7(8)
Hg3	Hg6	2.5248(13)	Hg6	O4	2.875(12)	O4	Cr1	O3	107.6(11)
Hg3	O6	2.569(15)	Hg6	O5	3.012(15)	O5	Cr1	O3	106.0(8)
Hg3	O2	2.666(13)	Hg6	O4	3.028(12)	O9	Cr1	O3	109.0(8)
O2	Hg1	Hg5	172.8(4)			O6	Cr2	O10	108.8(7)
O8	Hg2	O2	174.1(7)			O6	Cr2	O7	110.5(6)
O1	Hg3	Hg6	142.0(4)			O10	Cr2	O7	109.2(9)
O8	Hg4	O2	171.3(5)			O6	Cr2	O1	112.0(7)
O4	Hg5	Hg1	134.1(4)			O10	Cr2	O1	105.7(7)
O8	Hg6	Hg3	169.4(3)			O7	Cr2	O1	110.6(7)
Hg2	O2	Hg4	99.0(5)						
Hg2	O2	Hg1	112.6(6)						
Hg4	O2	Hg1	114.1(6)						
Hg2	O2	Hg3	117.9(6)						
Hg4	O2	Hg3	119.0(5)						
Hg1	O2	Hg3	95.1(5)						
Hg2	O8	Hg4	102.8(6)						
Hg2	O8	Hg6	114.4(6)						
Hg4	O8	Hg6	111.9(7)						
Hg2	O8	Hg5	122.9(7)						
Hg4	O8	Hg5	111.6(5)						
Hg6	O8	Hg5	93.6(5)						
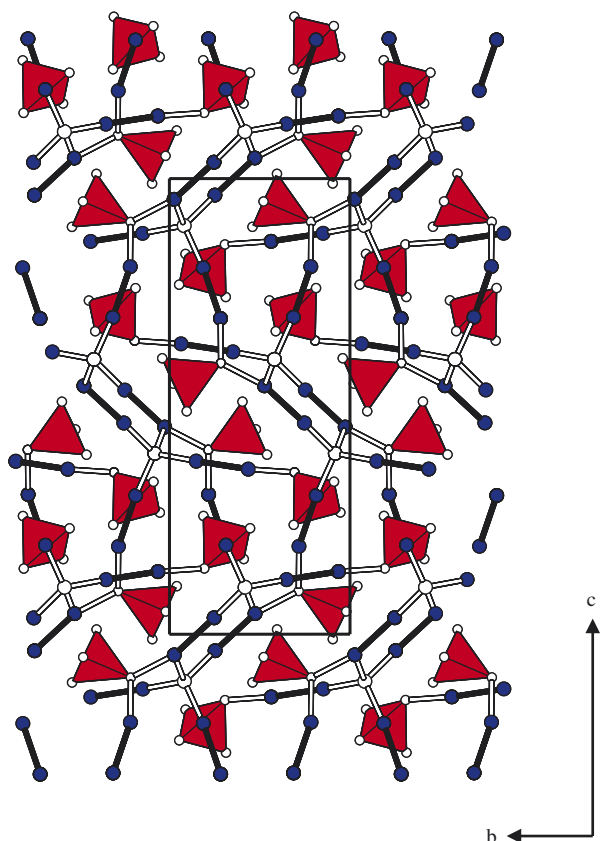
Fig. 1. (Color online) $Hg_6Cr_2O_9$. Crystal structure in projection along [100]. Hg atoms are displayed as (blue) light-grey spheres, O atoms as white spheres, and CrO_4 tetrahedra are given in the polyhedral representation (red online; dark-grey). For clarity, Hg–O bonds >2.5 Å have been omitted.

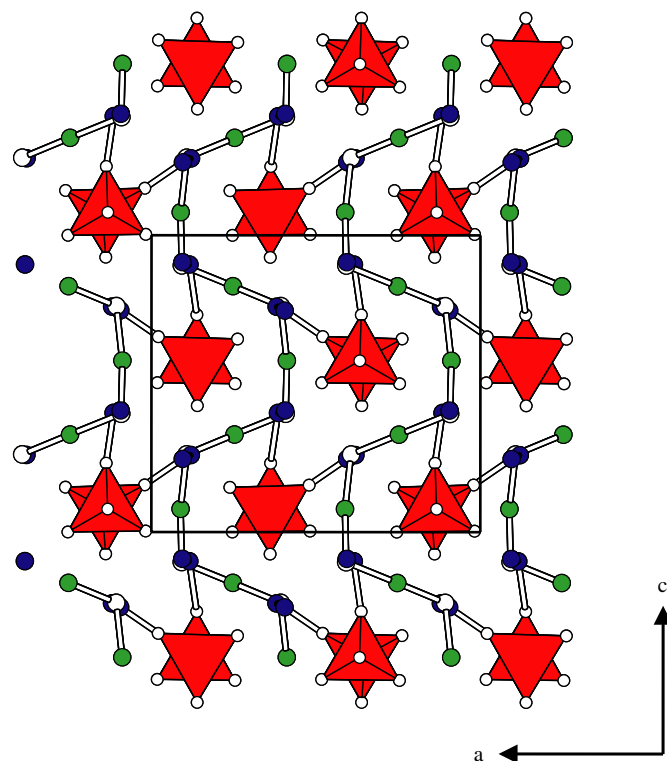Fig. 2. $Hg_6Cr_2O_9$. Details of the Hg–O network with thermal displacement parameters displayed at the 74% probability level.

Fig. 3. (Color online) $Hg_6Cr_2O_{10}$. Crystal structure in projection along [010]. Monovalent Hg atoms are displayed as (blue) light-grey spheres, divalent Hg atoms as (green) dark-grey spheres, O atoms as white spheres, and CrO_4 tetrahedra are given in the polyhedral representation (red online; dark-grey). For clarity, Hg–O bonds >2.4 Å have been omitted.

two O atoms tightly bonded to the dumbbell and Hg–O bond lengths between 2.1 and 2.4 Å. Except for two $\angle$(O–Hg–Hg) angles in $Hg_6Cr_2O_{10}$ (134.1(4)° for O4–Hg5–Hg1 and 142.0(4)° for O1–Hg3–Hg6), all other $\angle$(O–Hg–Hg) angles are nearly linear (Table 3). The two Hg^{2+} cations in $Hg_6Cr_2O_{10}$ (Hg2 and Hg4) exhibit a pronounced 2-coordination with two tightly bonded O atoms at distances around 2.07 Å and virtually linear $\angle$(O–Hg–O) angles. For the latter cations, the coordination spheres are augmented by four additional O atoms at considerably longer distances >2.65 Å, resulting in distorted octahedra as corresponding coordination polyhedra.

The single building blocks, [O–Hg–Hg–O] for the mercurous compound and [O–Hg–Hg–O] as well as [O–Hg–O] for the mixed-valent compound, are linked into intricate mercury–oxygen networks, details of which are displayed in Fig. 2 for $Hg_6Cr_2O_9$ and in Fig. 4 for $Hg_6Cr_2O_{10}$. In $Hg_6Cr_2O_9$, the [O–Hg–Hg–O] units generate a three-dimensional structure with the most outstanding feature of oxygen atom O5 tetrahedrally surrounded by Hg atoms, exhibiting Hg–O distances from 2.095(9) to 2.495(9) Å. The presence of such oxo-centered $[OHg_4]$ tetrahedra can be observed for various mercury oxocompounds and has recently been discussed in detail [26]. In $Hg_6Cr_2O_{10}$, the backbone of the mercury–oxygen network is made up of the [O–Hg–O] units that are linked to helical chains running parallel to the [001] direction. Single
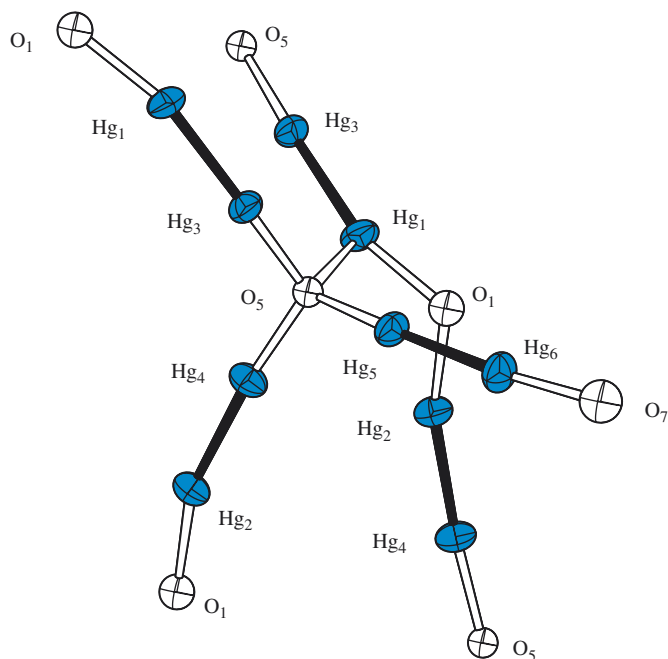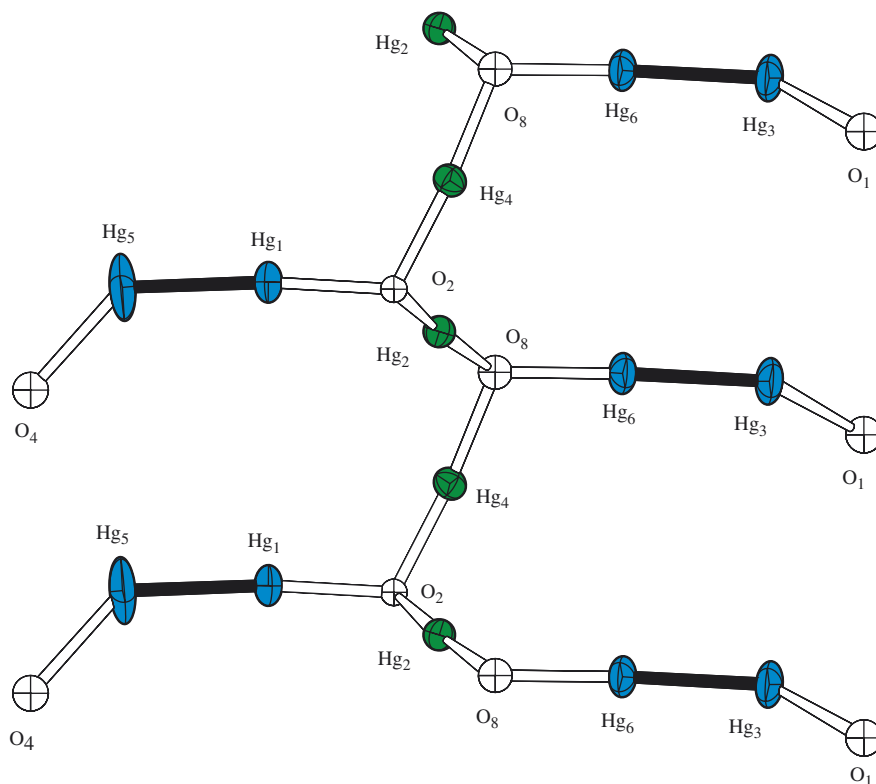
Fig. 4. (Color online) $Hg_6Cr_2O_{10}$. Details of the Hg–O network with thermal displacement parameters displayed at the 74% probability level. Monovalent Hg atoms are (blue) light-grey spheres, divalent Hg atoms are (green) dark-grey.

[O–Hg–Hg–O] blocks are catenated to this chain as branching units which leads to the formation of corrugated ribbons parallel to [001]. Adjacent ribbons are connected via more remote Hg–O contacts >2.4 Å into the three-dimensional structure. Similar to $Hg_6Cr_2O_9$, in $Hg_6Cr_2O_{10}$ oxo-centered [OHg$_4$] tetrahedra are observed for the oxygen atoms O2 and O8, however with a greater scattering of the Hg–O distances compared to the mercurous compound, here with Hg–O distances of 2.077(13) to 2.666(13) Å for O2, and of 2.045(13) to 2.932(14) Å for O8, respectively.

All CrO$_4$ tetrahedra have a slight angular distortion with intratetrahedral O–Cr–O angles deviating less than 4° from the ideal values. The average Cr–O distances are very similar, with values around 1.66 Å (Table 3), in close agreement with other mercury chromates(VI): Hg_5CrO_6 (1.689 Å) [7], $HgCrO_4 \cdot 2HgO$ (1.652 Å)^2 [9], $HgCrO_4 \cdot \frac{1}{2}H_2O$ (1.659 Å) [11], α-$HgCrO_4$ (1.652 Å), β-$HgCrO_4$ (1.649 Å), $HgCrO_4 \cdot H_2O$ (1.654 Å) [14]. The Cr1O$_4$ tetrahedron in $Hg_6Cr_2O_9$ exhibits the greatest scatter of Cr–O distances which range from 1.578(12) to 1.759(10) Å. This behaviour is caused by the different bond-valence requirements for the corresponding oxygen atoms. While the tightly bonded O9 atom has two additional mercury atoms as coordination partners at relatively long Hg–O distances around 2.8 Å, the O1 atom

with the longest Cr–O bond is bonded to two Hg atoms at much shorter Hg–O distances of 2.19 Å. A similar situation, however less pronounced, is found for the Cr2O$_4$ tetrahedron, with Cr–O distances between 1.620(11) and 1.719(12) Å. O8 with the shortest Cr–O bond is bonded to three Hg atoms at distances around 2.9 Å, whereas O7 with the longest Cr–O bond is coordinated by two Hg atoms, one with a very short Hg–O bond of 2.098(12) and one with a longer Hg–O bond of 2.689(11) Å. In the structure of $Hg_6Cr_2O_{10}$ the Cr–O bond lengths of the two CrO$_4$ tetrahedra are more regular, ranging from 1.644(16) to 1.699(15) Å.

The bond-valence sums (BVS) [29] for all metal atoms were calculated using the parameters by Brese and O'Keeffe [30]. They are close to the expected valence units (v.u.) for monovalent and divalent Hg, and for hexavalent Cr. $Hg_6Cr_2O_9$: Hg1 1.08, Hg2 1.06, Hg3 1.09, Hg4 1.10, Hg5 1.09, Hg6 1.08, Cr1 6.06, Cr2 5.75; $Hg_6Cr_2O_{10}$: Hg1 1.10, Hg2 1.96, Hg3 1.08, Hg4 1.96, Hg$_5$ 1.11, Hg6 1.02, Cr1 5.67, Cr2 5.64.

3.3. Thermal behaviour of $Hg_6Cr_2O_9$

The thermal decomposition of microcrystalline $Hg_6Cr_2O_9$ takes place in a four-step mechanism (Fig. 5). The compound is stable up to ca. 385 °C. Above this temperature a first decomposition range up to ca. 435 °C is observed, accompanied with two small endothermic effects

---

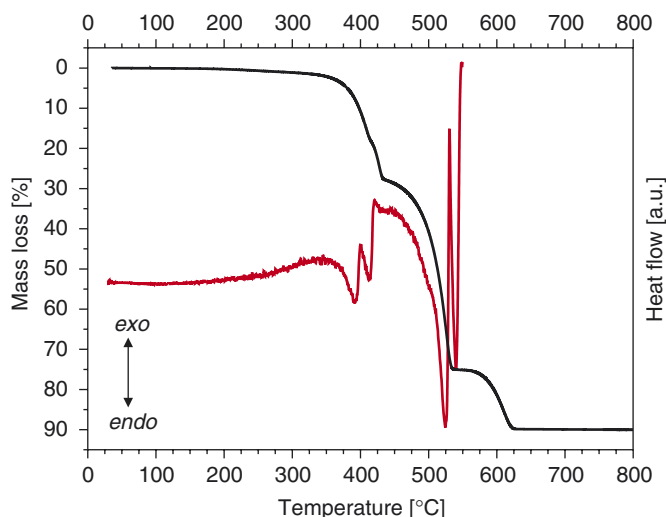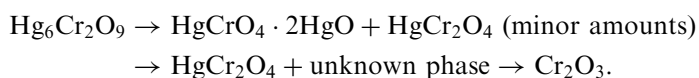^{2}The CrO$_4$ group in this structure is disordered around the twofold axis.

Fig. 5. (Color online) Thermal decomposition of $Hg_6Cr_2O_9$. The TG curve is displayed as a (black) dotted line, the DSC curve as a (red) solid line.

at 393 and 412 °C (note the slight shoulder in the corresponding TG curve). The observed mass loss of ca. 27% corresponds to a release of two Hg atoms per $Hg_6Cr_2O_9$ formula unit. XRPD of a sample heated to 430 °C under similar conditions, resulting in a dark brown powder, revealed $HgCrO_4 \cdot 2HgO$ [8] and traces of the spinel-type phase $HgCr_2O_4$ [11,15]. The second decomposition range is observed between 435 and 535 °C with a mass loss of ca. 64% (74% based on the original mass) and an intense endothermic DSC effect at 524 °C. XRPD of a sample heated up to 530 °C (dark-green to black powder) showed $HgCr_2O_4$ as the main phase, besides few reflections of a yet unknown phase in the system Hg–Cr–O. This phase has also been observed during thermal decomposition of mercury(II) dichromate(VI), $HgCr_2O_7$ [13]. Given a multiphase sample, the composition of this unknown phase could not, however, be determined reliably from energy-dispersive X-ray spectra. The determined Hg:Cr ratio showed a great variance with values between 1:3 and 1:5. The last decomposition reaction takes place between 535 and 625 °C, and a likewise intense endothermic DSC effect is observed at 538 °C. The mass loss of ca. 14% is conformed with a loss of the last Hg atom, and above 625 °C Cr_2O_3 is the only phase as detected by XRPD (green powder).

The main reaction products observed during the thermal decomposition of $Hg_6Cr_2O_9$ are summarised in the subsequent scheme:

$$Hg_6Cr_2O_9 \rightarrow HgCrO_4 \cdot 2HgO + HgCr_2O_4 \text{ (minor amounts)}$$
$$\rightarrow HgCr_2O_4 + \text{unknown phase} \rightarrow Cr_2O_3.$$

Although the observed mass loss of 89.5% based on the overall thermal decomposition reaction is in very good agreement with the theoretical mass loss of 89.53%

(Eq. (3)), the detailed mechanism of the intermediate product formation remains unclear:

$$Hg_6Cr_2O_{9,\,s} \rightarrow Cr_2O_{3,\,s} + 6Hg_{,\,g} \uparrow + 3O_{2,\,g} \uparrow. \qquad (3)$$

The thermolysis of $Hg_6Cr_2O_9$ involves several redox-reactions, including the redox-pairs Hg^0/Hg^I, Hg^0/Hg^{II}, Hg^I/Hg^{II}, Cr^{III}/Cr^{VI} and O^0/O^{-II}. For a more detailed insight into these redox-reactions and the corresponding phase equilibria, temperature-dependent XRPD measurements and TG/DSC experiments coupled with mass-spectrometric or vibrational spectroscopic measurements are planned for the future.

References

[1] K. Brodersen, G. Göbel, G. Liehr, Z. Anorg. Allg. Chem. 575 (1989) 145–153.
[2] G.V. Romanenko, S.V. Borisov, J. Struct. Chem. 41 (2000) 888–889.
[3] M. Weil, Z. Naturforsch. 56b (2001) 753–758.
[4] A.L. Wessels, W. Jeitschko, M.H. Moeller, Z. Naturforsch. 52b (1997) 469–473.
[5] M. Weil, R. Glaum, J. Solid State Chem. 157 (2001) 68–75.
[6] M. Weil, Z. Kristallogr. 219 (2004) 621–629.
[7] L.A. Groat, A.C. Roberts, Y. Le Page, Can. Mineral. 33 (1995) 41–46.
[8] Gmelins Handbuch der anorganischen Chemie, vol. 52, Chrom, Part B, Verlag Chemie, Weinheim, Germany, 1962, p. 875 f.
[9] T. Hansen, Hk. Müller-Buschbaum, L. Walz, Z. Naturforsch. 50b (1995) 47–50.
[10] C. Stålhandske, Acta Crystallogr. B 34 (1978) 1968–1969.
[11] K. Aurivillius, C. Stålhandske, Z. Kristallogr. 142 (1975) 129–141.
[12] A.L. Wessels, R. Czelalla, W. Jeitschko, Mater. Res. Bull. 33 (1998) 95–101.
[13] M. Weil, B. Stöger, E.J. Baran, Monatsh. Chem. (2006) accepted for publication.
[14] B. Stöger, M. Weil, Z. Naturforsch. 61b (2006) accepted for publication.
[15] M. Weil, B. Stöger, Acta Crystallogr. E 62 (2006) submitted for publication.
[16] W. Herrendorf, HABITUS, Program for Optimisation of the Crystal Shape for the Numerical Absorption Correction, Universities of Karlsruhe and Gießen, Germany, 1993/1997.
[17] G.M. Sheldrick, SHELXTL (version 6.10.), Bruker AXS Inc., Madison, WI, USA, 2001.
[18] L.M. Gelato, E. Parthé, J. Appl. Crystallogr. 20 (1987) 139–143.
[19] A.K. Spek, J. Appl. Crystallogr. 36 (2003) 7–13.
[20] H. Flack, G. Bernardinelli, Acta Crystallogr. A 55 (1999) 908–915.
[21] E. Dowty, Atoms for Windows (version 6.1), Shape Software, 521 Hidden Valley Road, Kingsport, TN 37663, USA, 2004.
[22] F. Fichtner, G. Oesterheld, Z. Anorg. Allg. Chem. 76 (1912) 347–356.
[23] M. Weil, Solid State Sci. 4 (2002) 1153–1162.
[24] Handbook of Chemistry and Physics, 76th ed., CRC Press, Boca Raton, FL, 1995.
[25] N.V. Pervukhina, S.A. Magarill, S.V. Borisov, G.V. Romanenko, N.A. Pal'chik, Russ. Chem. Rev. 68 (1999) 615–636.
[26] S.V. Borisov, S.A. Magarill, N.V. Pervukhina, E.V. Peresypkina, Crystallogr. Rev. 11 (2005) 87–123.
[27] S.V. Borisov, S.A. Magarill, N.V. Pervukhina, J. Struct. Chem. 45 (2004) 446–453.
[28] M. Weil, E. Tillmanns, D. Yu. Pushcharovsky, Inorg. Chem. 44 (2005) 1443–1451.
[29] I.D. Brown, The Chemical Bond in Inorganic Chemistry, Oxford University Press, Oxford, 2002.
[30] N.E. Brese, M. O'Keeffe, Acta Crystallogr. B 47 (1991) 192–197.